Journal of Sustainable Metallurgy (2026) 12:142–156
https://doi.org/10.1007/s40831-025-01298-7

RESEARCH ARTICLE

Investigation of Methanesulfonic Acid as a Novel Leaching Agent for Metal Recovery from Municipal Solid Waste Incineration Fly Ash

Edzhe Soylu[1] · Linus Meistad[1] · Elif Emil-Kaya[1] · Kai Erik Ekstrøm[2] · Inge Johansson[2] · Przemyslaw B. Kowalczuk[3] · Gabriella Tranell[1]

Received: 16 April 2025 / Accepted: 29 September 2025 / Published online: 17 October 2025

Abstract

This study investigates the efficiency of methanesulfonic acid (MSA) as an alternative, environmentally benign leaching agent for extracting metals from municipal solid incineration fly ash (MSWI FA). A series of experiments were conducted to evaluate the effects of key leaching parameters, including ash type, solid-to-liquid ratio, MSA concentration and temperature, on the leachability of metals. MSA combined with 1 vol.% H_2O_2 achieved 96.47 ± 4.3%, 89.52 ± 4.3%, and 45.89 ± 5.1% for Cu, Zn, and Pb, respectively. Pb extraction was significantly enhanced by elevated temperatures and higher acid concentrations. Leaching efficiencies for economically valuable elements such as Cu and Zn remained consistently high across all ash types, indicating their broad solubility. In contrast, the extraction of elements like Pb, Ni, and Cr showed greater variability depending on the ash type, likely due to differences in metal speciation and phase associations. The conductivity of MSA solutions ranged from 0.25 to 0.34 S/cm, indicating suitability for electrowinning applications with minimal pre-treatment. Overall, the results demonstrate that MSA is an effective and competitive leaching agent for the recovery of Cu, Zn, and Pb from MSWI FA, offering performance and cost advantages comparable to other bulk organic acids.

Graphical Abstract

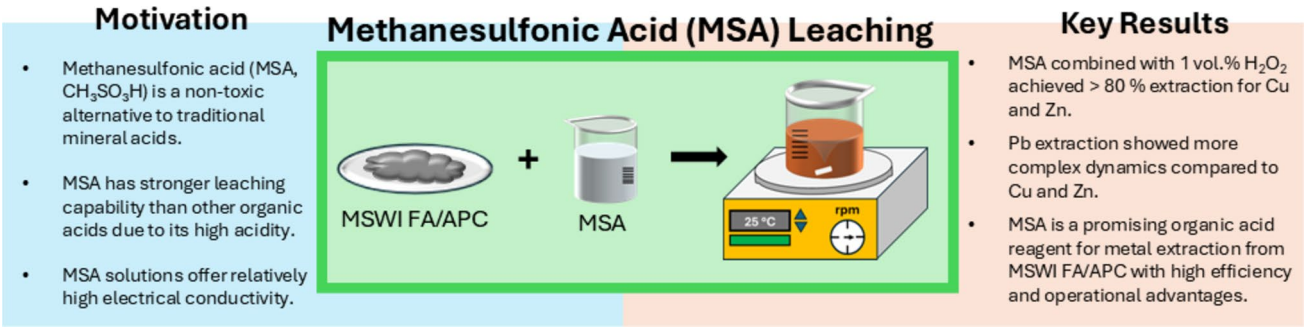

Keywords Hydrometallurgical extraction · Sustainable acid · Resource recovery · Leaching kinetics · Metal speciation

The contributing editor for this article was Nikhil Dhawan.

✉ Edzhe Soylu
ece.soylu@ntnu.no

[1] Department of Materials Science and Engineering, Norwegian University of Science and Technology (NTNU), Alfred Getz Vei 2B, 7041 Trondheim, Norway

[2] NOAH AS, Langgata 48, 3080 Holmestrand, Norway

[3] Department of Geosciences, Norwegian University of Science and Technology (NTNU), S.P. Andersens Vei 15A, 7031 Trondheim, Norway

Introduction

Global municipal solid waste (MSW) production is projected to reach 3.4 billion tones by 2050, driven by population growth and increasing GDP per capita [1]. Among the waste treatment methods, municipal solid waste incineration (MSWI) has become a key waste management strategy due to its ability to reduce waste volume by 85–90%, and eliminate organic matter [2, 3]. MSWI primarily relies on

three types of incinerators: grate furnaces (GF), fluidized bed furnaces (FB), and rotary kilns (RK). In Europe, GF is the most common, used in about 90% of facilities, while FB and RK account for approximately 5% and 2%, respectively [4]. The primary distinctions among these technologies are their combustion processes and operating temperatures. GF and RKs typically operate at high temperatures (~ 1100 °C), whereas FB systems function at a lower temperature range of 700–900 °C [5].

Fly ash (FA), a byproduct of the incineration process, is categorized as hazardous due to its high concentrations of leachable heavy metals and other toxic substances [6–10]. This fine particulate material is collected from combustion gases before they pass through the flue gas cleaning system [11]. To enhance pollution control, sorbents or chemical reagents are often introduced into the flue gas, leading to the production of air pollution control (APC) residues, which are frequently combined with FA [12]. Currently, the predominant waste management strategy involves landfilling stabilized FA/APC. However, with growing environmental concerns and the implementation of new directives (e.g. Directive (EU) 2018/850 [13]) that limits landfilling, the focus has shifted towards developing effective utilization of FA/APC as a more sustainable alternative to disposal [1, 13–15].

A typical mineralogical composition of MSWI FA includes Ca-based compounds ($Ca(OH)_2$, CaClOH, $CaCO_3$, $CaSO_4$), chloride salts (NaCl, KCl), quartz, and amorphous phases. The major constituent elements of FA are Ca, Cl, Si, Al, K, Na, and S, with the high calcium content attributed to the use of $Ca(OH)_2$ in flue gas desulfurization. MSWI fly ash also contains heavy metals such as Zn, Pb, Cu, Cr, Cd, and Ni, where they primarily occur as oxides, carbonates, hydroxides, and chlorides [7, 12, 16]. Characterization studies reveal that Cu predominantly exists as CuCl, CuO, and $Cu(OH)_2$, with relatively consistent speciation across samples, whereas Zn primarily occurs as K_2ZnCl_4, $ZnFe_2O_4$, and $Zn_5(CO_3)_2(OH)_2$, displaying greater variability across different ashes [17, 18].

Metals like Zn and Cu, which are vital for various industries, are increasingly targeted for recovery from various waste streams due to their limited supply and high economic value. With Zn and Cu concentrations comparable to those found in natural ore, MSWI fly ash emerges as additional source for metals [19]. On the other hand, leaching Pb from MSWI FA/APC is essential to reduce its environmental toxicity, comply with regulatory limits, and enable safe disposal or potential reuse of the treated ash. To date, the state-of-the-art method for extracting metals from MSWI FA is the FLUgaschen-WAschen (FLUWA) process, which utilizes scrub water from wet flue gas cleaning with added HCl for pH adjustment [20]. Currently, over 60% of Switzerland's fly ash is processed through the FLUWA process [21, 22]. Although effective, the reliance on mineral acids like HCl poses environmental and economic challenges, including hazardous by-product generation and high waste treatment costs. Consequently, common organic acids such as acetic and citric acid have emerged as potentially more sustainable alternative, demonstrating efficient extraction of metals like Cu and Zn (50%–90%), although Pb leaching efficiencies remain relatively low due the stability of Pb-compounds, typically below 30% [23, 24].

Methanesulfonic acid (MSA, CH_3SO_3H) stands out as a non-toxic alternative to conventional mineral acids such as hydrochloric, sulfuric and nitric acid [25]. Its biodegradability and low environmental impact make spent MSA easier to handle and dispose of than mineral acids. Compared to other organic acids, MSA exhibits superior leaching capability with a strong acidity ($pKa = -1.9$) [26]. One of MSA's key advantages lies in the relatively high electrical conductivity of its aqueous solutions (0.59×10^{-3} S/cm), which is significantly higher than that of traditional organic acids and, while lower than strong mineral acids, is still sufficient to support electrochemical processes [25, 26]. This conductivity potentially enables direct electrochemical recovery of metals from leachate solutions without requiring additional supporting electrolytes, thereby reducing reagent use and making the process more cost-effective and energy-efficient compared to conventional methods such as solvent extraction. Moreover, recent advancements in the regeneration and reuse of MSA further enhance its potential within closed-loop hydrometallurgical systems, supporting circular hydrometallurgy strategies [26]. In addition, MSA's ability to effectively dissolve a wide range of metal compounds—including oxides, hydroxides, and carbonates—makes it ideal for treating complex matrices such as MSWI fly ash. Notably, MSA has demonstrated superior efficiency in dissolving Pb compared to sulfuric or hydrochloric acids, due to the poor solubility of Pb sulfates and chlorides.

Several studies showed that MSA effectively extracts metals from various sources, including primary and secondary raw materials. Palden et al. [27] recovered Pb (100%), Zn (50%), and Fe (20%) from jarosite using MSA, with higher temperatures (up to 160 °C) enhancing Zn leaching. Jadhao et al. [28] extracted Cu, Zn, and Ni from printed circuit boards using 1 M MSA and 1 M H_2O_2, achieving nearly complete Cu and Zn recovery and 80% Ni recovery at 40 °C and a 2-h leaching time. Increasing MSA concentration beyond 1 M had no further benefit, and 0.6 M H_2O_2 was optimal. Ahn et al. [29] showed that MSA with H_2O_2 improved Cu recovery from chalcopyrite (60–90%), with efficiency increasing at 75 °C and longer leaching times (up to 100 h). Wu et al. [30] recovered 98% Pb from cerussite concentrate (67.12% Pb) via MSA leaching, demonstrating scalability with solid densities from 20 to 200 g/L.

Numerous studies have investigated kinetic models to understand the leaching behavior of FA. Among these, the shrinking core model (SCM), widely used for solid–liquid systems, has been applied to describe the leaching of metals from MSWI fly ash. Caviglia et al. [31] demonstrated that diffusion through the product layer is the dominant mechanism, supported by low activation energies, indicative of diffusion control. Additionally, an empirical second-order model ($R^2 > 0.98$) identified a two-step leaching process: an initial rapid surface dissolution phase followed by a slower, diffusion-driven release. Higher temperatures (80 °C) were found to enhance leaching rates but did not alter the underlying diffusion-controlled mechanism, highlighting diffusion as the primary rate-limiting factor. Meer and Nazir [32] reported pseudo-first-order kinetics for metals like Al, Fe, and Zn, indicating dependency on the concentration of the unreacted solid, while Pb followed second-order kinetics. Luo et al. [33] showed leaching mechanisms in MSWI ash were governed by solubility and sorption controls. Solubility-driven leaching involves the dissolution of metal oxides (e.g., ZnO, Al_2O_3), influenced by pH-dependent precipitation and secondary phase formation, while sorption mechanisms regulate the release of metals like Pb and Cu through adsorption onto ash surfaces or complexation with dissolved organic matter. Kinetics were primarily dictated by particle size, with smaller fractions exhibiting faster leaching due to higher surface area and reactivity.

To the best of the authors' knowledge, MSA has not yet been studied for the extraction of metals such as Cu, Zn, and Pb from MSWI FA/APC, and its application to this waste stream remains largely unexplored. The aim of the current study is to optimize MSA leaching conditions to extract Cu, Zn and Pb, as well as determining the leachability of other minor elements from different types of MSWI FA, and to discuss its future use in MSWI FA valorization.

Materials and Methods

Materials

The FA/APC samples used in this study were collected from various incineration plants in Scandinavia, comprising five types: rotary kiln ash (Ash A), grate furnace ashes (Ash B, Ash C, and Ash D), and circular fluidized bed ash (Ash E). Except for Ash A and Ash D, all samples were a blend of FA/APC ashes. Additionally, Ash A was distinct as it is a mixture of 95% industrial waste and 5% municipal solid waste. The samples were provided by NOAH AS, a waste treatment company in Norway, and delivered in large barrels (60–80 kg). These were then divided into 250-g portions using universal splitters in a stepwise process. Before the experiments, the samples were water-washed to eliminate soluble salts and then dried overnight at 80 °C. The dried samples were then analyzed for elemental composition using Inductively Coupled Plasma Mass Spectrometry (ICP-MS). A detailed characterization of these ashes, including mineralogical and morphological analyses, is available in a separate publication [34]. The results showed that water washing removed most soluble salts (24.2–54.4 wt.% mass loss across ash types) and enriched wash waters in Na, K, Ca, S, and trace metals (Cu, Pb, Zn), consistent with dissolution of easily soluble salts (e.g., NaCl, KCl) and some metal sulfates/chlorides. In this work, Table 1 summarizes the elemental composition of the washed samples, with mean values and standard deviations from replicate measurements; the corresponding concentration data from the specific sample bag used in this study for calculations are given in Table S1. Particle size distribution (PSD), measured with a Horiba Partica LA-960 analyzer, is presented in Table 2.

Methods

An experimental design following a one-variable-at-a-time (OVAT) approach with center point replication was employed to assess the influence of individual factors on metal extraction. The matrix (Table 3) investigated the effects of methanesulfonic acid (MSA, 70 wt.% in H_2O, Merck®) concentration (1 M, 2 M, 3 M), temperature (20 °C, 40 °C, 60 °C), and solid-to-liquid (S/L) ratio (1/10, 1/20, 1/30) on metal extraction efficiency. Ash E was selected for parameter screening due to its relatively high Cu content, making it a suitable reference for evaluating MSA leaching. The identified central condition (2 M MSA, 40 °C, 1/20 S/L) was then applied to Ashes A–D to assess the robustness and transferability of the approach across different ash types. MSA leaching was tested both with 1 vol.% of H_2O_2 (30%, EMSURE®) and without an oxidant to determine the effect of oxidant in leaching of different elements. Leaching was conducted in Erlenmeyer flasks (300 ml) on top of thermostat heating elements with magnetic stirring at 300 rpm. Lenses were placed on top of the flasks to prevent liquid loss from evaporation to maintain consistent conditions. Samples were collected at 0.5 h, 1 h, 2 h, 3 h, and 4 h intervals, with 1 ml of filtered leachate (0.45 µm PTFE syringe) diluted to 10 ml and analyzed via ICP-MS (Perkin Elmer Elan DRC-II). The final pH of the solutions was determined as highly acidic (pH = ~ 1). Extraction efficiencies were determined by comparing the metal mass found in the leachates to the metal mass in the ash before leaching (Eq. 1).

$$\text{Extraction}\,(\%) = \frac{C_{\text{leachate}} \times V_{\text{leachate}}}{C_{\text{initial}} \times m_{\text{solid}}} \times 100 \quad (1)$$

where,

Table 1 Average concentrations (wt.%) and standard deviations (±) of major and trace elements in five different MSWI fly ash samples (Ash A–E). Values represent the mean ± standard deviation from replicate measurements

Element	Ash A	Ash B	Ash C	Ash D	Ash E
	wt.% ± STD				
Al	3.300 ± 0.173	4.197 ± 3.044	3.798 ± 3.044	4.475 ± 0.254	10.370 ± 0.998
As	0.042 ± 0.003	0.001 ± 0.001	0.006 ± 0.001	0.012 ± 0.002	0.003 ± 0.002
Ba	2.576 ± 1.522	0.136 ± 0.031	0.109 ± 0.031	0.340 ± 0.009	0.213 ± 0.005
Ca	6.553 ± 0.175	30.267 ± 6.389	29.581 ± 6.389	23.883 ± 1.179	22.560 ± 0.741
Cd	0.003 ± 0.001	0.017 ± 0.002	0.022 ± 0.002	0.005 ± 0.001	0.004 ± 0.001
Co	0.030 ± 0.001	0.002 ± 0.000	0.005 ± 0.000	0.004 ± 0.000	0.009 ± 0.000
Cr	0.140 ± 0.020	0.043 ± 0.022	0.029 ± 0.022	0.066 ± 0.006	0.040 ± 0.007
Cu	0.555 ± 0.058	0.085 ± 0.011	0.101 ± 0.011	0.082 ± 0.005	0.620 ± 0.114
Fe	4.597 ± 1.577	1.597 ± 0.723	1.593 ± 0.723	2.203 ± 0.362	2.339 ± 0.243
K	2.773 ± 0.729	0.509 ± 0.106	0.360 ± 0.106	0.643 ± 0.029	0.330 ± 0.159
Mg	1.100 ± 0.105	1.240 ± 0.251	1.329 ± 0.251	1.895 ± 0.100	2.307 ± 0.656
Mn	0.296 ± 0.006	0.071 ± 0.015	0.098 ± 0.015	0.147 ± 0.011	0.125 ± 0.011
Mo	0.156 ± 0.086	0.003 ± 0.003	0.002 ± 0.003	0.004 ± 0.001	0.002 ± 0.000
Na	7.103 ± 0.650	0.519 ± 0.160	0.611 ± 0.160	0.811 ± 0.114	0.749 ± 0.299
Ni	0.209 ± 0.001	0.006 ± 0.002	0.015 ± 0.002	0.012 ± 0.002	0.016 ± 0.001
P	10.610 ± 1.621	0.582 ± 0.248	0.743 ± 0.248	0.831 ± 0.102	0.332 ± 0.168
Pb	0.676 ± 0.206	0.185 ± 0.057	0.187 ± 0.057	0.237 ± 0.032	0.262 ± 0.045
S	0.888 ± 0.576	2.937 ± 0.836	5.133 ± 0.836	9.167 ± 1.607	2.070 ± 0.376
Sb	0.029 ± 0.039	0.025 ± 0.032	0.078 ± 0.032	0.111 ± 0.068	0.019 ± 0.024
Si	4.170 ± 3.620	5.340 ± 5.498	6.984 ± 5.498	8.031 ± 0.471	7.523 ± 6.551
Sn	0.094 ± 0.086	0.038 ± 0.033	0.078 ± 0.033	0.029 ± 0.003	0.020 ± 0.019
Ti	1.470 ± 1.264	0.597 ± 0.451	0.949 ± 0.451	1.527 ± 0.064	1.187 ± 0.720
Zn	5.403 ± 1.020	1.257 ± 0.051	1.467 ± 0.051	2.233 ± 0.058	0.634 ± 0.037

Table 2 Particle size distribution of the ash samples

	d10 (μm)	d50 (μm)	d90 (μm)
Ash A	1.9	14.0	124.0
Ash B	3.6	13.7	97.9
Ash C	3.2	27.1	168.0
Ash D	9.1	54.2	216.0
Ash E	4.2	21.6	74.2

$C_{leachate}$ = metal concentration in leachate (mg/L).
$L_{eachates}$ = leachate volume (L).
$C_{initial}$ = initial solid-phase metal content (mg/kg).
M_{solid} = solid sample mass (kg).

Results and Discussion

MSA is not an oxidizing acid; therefore, it cannot directly dissolve less reactive metals, particularly precious metals, and necessitates the addition of an oxidizing agent. However, MSA readily dissolves metal oxides, hydroxides, and carbonates, forming soluble methanesulfonate salts [35]. As summarized in Table 4, the speciation of Cu, Zn, and Pb in FA/APC enables their classification into three groups: (I) readily soluble forms (e.g., oxides, hydroxides, carbonates), (II) zero-valent metals, and (III) poorly soluble or inert phases such as spinels, sulfides, and silicates. In this study, the ash samples were water-washed prior to leaching, resulting in the removal of most chlorine-bearing compounds. Only Cu and Zn are reported to be found metallic, and due to the high reactivity of Zn it is readily soluble in MSA. Equations (2), (3), (4), (5), (6), (7), (8), (9), and (10) present the dominant reactions expected between MSA and the identified compounds.

Readily Leachable Compounds

These include common oxidized forms of Cu, Zn, and Pb such as oxides, hydroxides, and carbonates. MSA reacts directly with these species to form soluble methanesulfonate salts:

Copper compounds:

$$CuO + 2CH_3SO_3H \rightarrow Cu\left(CH_3SO_3\right)_2 + H_2O \quad (2)$$

Table 3 Experimental design matrix showing the tested parameters in the leaching experiments. The experiments are grouped based on the investigated variable: acid concentration, temperature, S/L ratio, H_2O_2 effect, and ash type

Experiment number	Ash	S/L	T (°C)	C (M)	H_2O_2 (vol.%)
Concentration					
1	E	1/20	40	1	1
2	E	1/20	40	2	1
3	E	1/20	40	3	1
Temperature					
4	E	1/20	20	2	1
2	E	1/20	40	2	1
5	E	1/20	60	2	1
S/L					
6	E	1/10	40	2	1
2	E	1/20	40	2	1
7	E	1/30	40	2	1
Effect of H_2O_2					
2	E	1/20	40	2	1
8	E	1/20	40	2	0
Parallels					
9	E	1/20	40	2	1
10	E	1/20	40	2	1
11	E	1/20	40	2	1
Ash type					
12	A	1/20	40	2	1
13	B	1/20	40	2	1
14	C	1/20	40	2	1
15	D	1/20	40	2	1

Table 4 Cu, Zn, and Pb speciation in MSWI FA/APC samples. Results from various XANES studies in literature

Metal	Compound forms in MSWI FA/APC
Cu	Cu (metallic) [17, 36–38], CuCl/$CuCl_2$ [17], CuO [36, 38, 39], $Cu(OH)_2$ [17, 36], $CuCO_3$ [36], $CuSiO_3{\cdot}H_2O$ [17], $CuFe_2O_4$ [17], $CuSO_4/CuSO_4.5H_2O$ [17, 38, 39], CuClOH [38], $Cu_3(PO_4)_2$ [38], Cu_2S [38]
Zn	K_2ZnCl_4 [18, 40], **$ZnFe_2O_4$ [17, 18, 40], $ZnAl_2O_4$ [17, 18, 40, 41], $Zn_5(CO_3)_2(OH)_6$ [17, 18, 41], $ZnSiO_4$ [40, 41], $Zn_4Si_2O_7(OH)_2{\cdot}H_2O$ [17, 18], $ZnCl_2$ [17, 40, 42], ZnO/$Zn(OH)_2$ [17], $Zn_5(OH)_8Cl_2.H_2O$ [18], Zn (surface adsorbed) [18]
Pb	$PbCl_2$ [42, 43], PbO [42, 43], PbS [42], $PbCO_3$ [42], PbO_2 [42]

$$Cu(OH)_2 + 2CH_3SO_3H \rightarrow Cu\left(CH_3SO_3\right)_2 + 2H_2O \quad (3)$$

$$CuCO_3 + 2CH_3SO_3H \rightarrow Cu\left(CH_3SO_3\right)2 + H_2O + CO_2 \quad (4)$$

Zinc compounds:

$$ZnO + 2CH_3SO_3H \rightarrow Zn\left(CH_3SO_3\right)2 + H_2O \quad (5)$$

$$Zn(OH)_2 + 2CH_3SO_3H \rightarrow Zn\left(CH_3SO_3\right)_2 + 2H_2O \quad (6)$$

$$Zn_5\left(CO_3\right)_2(OH)_6 + 10CH_3SO_3H \rightarrow 5Zn\left(CH_3SO_3\right)2 + 2CO_2 + 8H_2O \quad (7)$$

Lead compounds:

$$PbO + 2CH_3SO_3H \rightarrow Pb\left(CH_3SO_3\right)_2 + H_2O \quad (8)$$

$$PbCO_3 + 2CH_3SO_3H \rightarrow Pb\left(CH_3SO_3\right)2 + CO_2 \uparrow + H_2O \quad (9)$$

Metallic Forms (Oxidizing Agent Required)

In comparison to metallic Zn, zero-valent Cu and Pb are more noble and do not dissolve in MSA alone. However, in the presence of an oxidizing agent such as hydrogen peroxide (H_2O_2), they can be oxidized and then solubilized as methanesulfonates:

$$CuO + H_2O_2 + 2CH_3SO_3H \rightarrow Cu\left(CH_3SO_3\right)2 + 2H_2O \quad (10)$$

Stable or Acid-Resistant Phases

Certain crystalline and thermodynamically stable phases identified in MSWI FA/APC, including spinel-type oxides (e.g., $CuFe_2O_4$, $ZnFe_2O_4$, $ZnAl_2O_4$), silicates (e.g., $CuSiO_3{\cdot}H_2O$, Zn_2SiO_4), and sulfides (e.g., Cu_2S, PbS), are not significantly soluble in MSA alone. While these species are largely retained in the leaching residue under standard conditions, dissolution can be achieved using an oxidizing agent in combination with elevated temperature, increased residence time, or with the presence of stronger redox couples.

Effect of H_2O_2 and Time on the Leachability of the Metals

Figure 1 illustrates the varying effects of H_2O_2 on the leaching behavior of metals in Ash E under center-point leaching conditions, with a notable improvement observed only for Cu, where the extraction efficiency rises sharply from below 10% to 97.6% (Table S2). The observed enhancement in Cu leachability with H_2O_2, reaching its maximum at 4 h, correlates well with reports showing that oxidation facilitates the conversion of the less soluble Cu^+ to the more soluble Cu^{2+} species, thereby improving its solubility [28, 29]. This suggests Cu is found in stable compound forms such

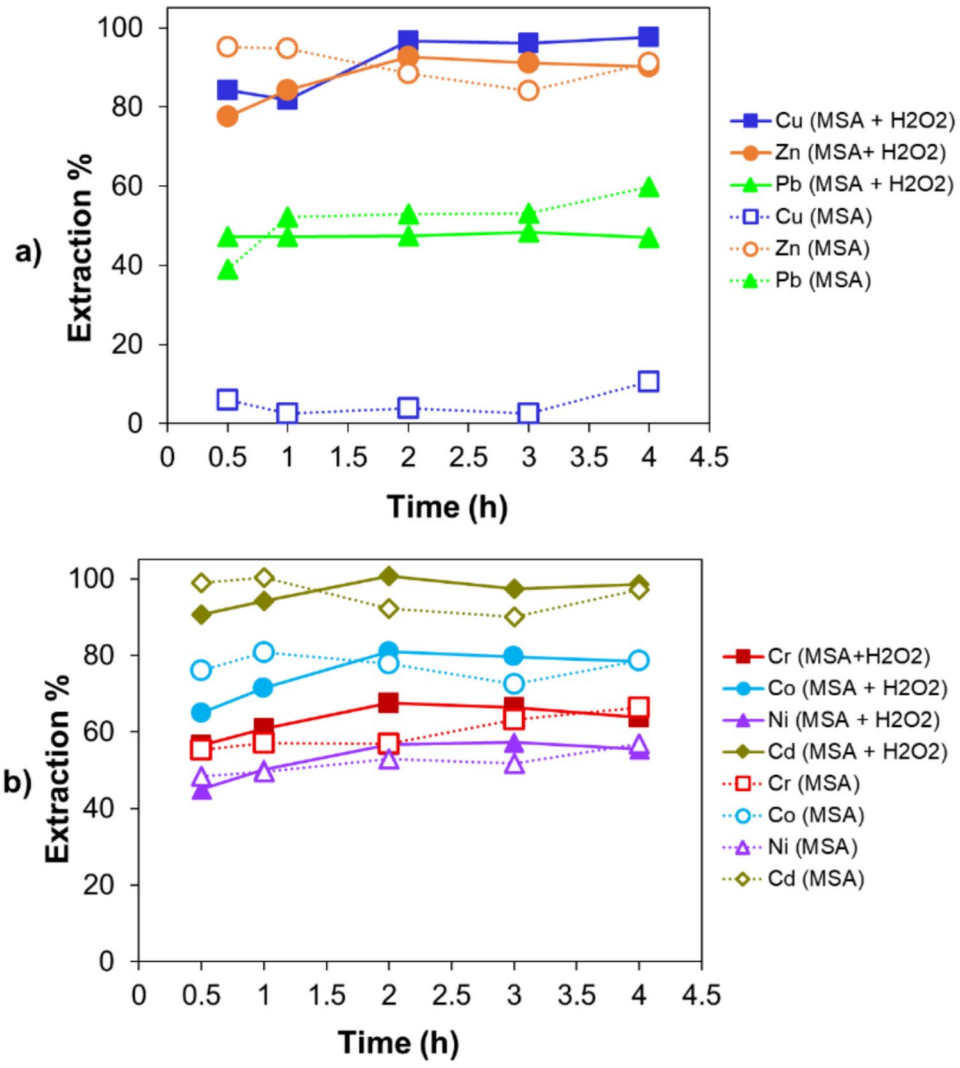

Fig. 1 Extraction % of **a** Cu, Zn, and Pb and **b** Cr, Co, Ni, and Cd in the leaching solution with time. Based on central parameters (1/20 S/L ratio, 40 °C, 2 M MSA) with and without 1 vol.% H_2O_2, using Ash E. For MSA + H_2O_2 values, an average of 3 parallel experiments is used

as $CuSiO_3{\cdot}H_2O$, $CuFe_2O_4$, $CuSO_4/CuSO_4.5H_2O$ or Cu_2S. Except during the initial stage of leaching, where kinetic equilibrium has not yet been fully established, Zn exhibited relatively stable leachability regardless of the presence of an oxidizing agent. This behavior reflects the predominance of Zn^{2+} in acid-soluble forms such as ZnO, $ZnCl_2$, or surface-adsorbed Zn species. While oxidizing agents do not directly affect the oxidation state of Zn, they may indirectly influence its solubility by modifying the dissolution behavior of associated compounds or altering the pH of the leaching environment. For example, they can enhance the solubility of Zn-bearing sulfides or oxides, thereby facilitating Zn release into solution [44, 45]. The leaching behavior of Cr, Co, Ni, and Cd in the presence and absence of H_2O_2 closely mirrored that of Zn, suggesting these elements may share similar mineral associations within the ash matrix and exhibit comparable leaching kinetics.

Adding H_2O_2 to MSA did not enhance Pb extraction; instead, the efficiency decreased from 59.79% with MSA alone to 46.97% at 4-h mark when combined with H_2O_2. Water washing effectively removes water soluble phases, where present, a fraction of soluble Pb species (e.g., $PbCl_2$) may be co-dissolved, leaving behind more sparingly soluble forms. MSA alone efficiently dissolves PbO and $PbCO_3$. Conversely, PbS is resistant to dissolution in non-oxidizing environments but may oxidize in the presence of H_2O_2, potentially forming $PbSO_4$, which is insoluble in MSA. Indeed, industrial electrowinning processes using MSA avoids $PbSO_4$ due to its inadequate solubility. Consequently, any formation of $PbSO_4$ during oxidizing extraction would hinder Pb recovery and explain the observed decline in extraction efficiency with H_2O_2 [35, 46]. The presence of the oxidant had a limited impact on trace metals, as extraction efficiencies after 4 h were comparable under both MSA and MSA + H_2O_2 conditions.

Effect of S/L Ratio, Temperature and Acid Concentration on Leachability

Figure 2 shows the influence of various parameters (S/L ratio, temperature, and acid concentration) on the leaching efficiency of the different elements. These findings highlight the critical role of the S/L ratio. A decrease from 1/10 to 1/20 led to a substantial improvement in extraction efficiency across all elements, likely due to increased reagent availability per unit mass of solid and improved mass transfer. However, further reduction to 1/30 resulted in limited additional benefits, with the most notable increase observed for Pb and a decline observed for Cu and Cd. This suggests that while lower S/L ratios can enhance leaching by minimizing local saturation and improving dispersion, excessively low solid loadings may also introduce dilution effects that limit reaction kinetics or reduce the driving force for leaching for certain elements.

Temperature exhibited a comparatively minor influence on overall metal extraction. While most elements showed limited response to temperature variation, notable increases in extraction were observed for Pb, Cr, and Co at 60 °C, indicating enhanced dissolution under elevated thermal conditions. Interestingly, a slight reduction in extraction efficiencies was observed for Pb and Cd when the temperature was increased from room temperature to 40 °C.

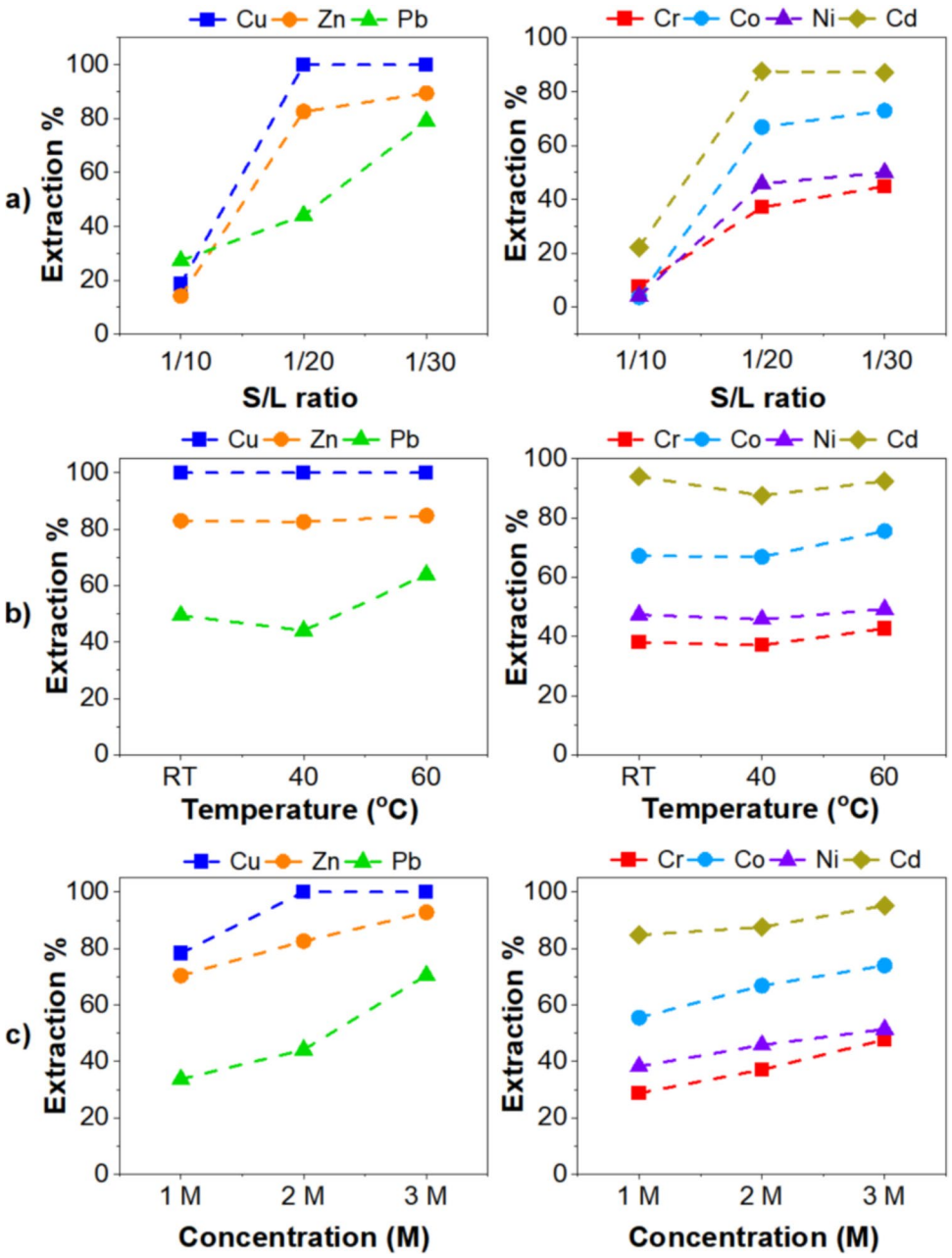

Fig. 2 Effect of **a** solid-to-liquid ratio, **b** temperature, and **c** MSA concentration on the leaching concentrations of Cu, Zn, Pb, Cr, Co, Ni, and Cd, using Ash E. For each parameter tested other parameters as follows: **a** 2 M MSA + 1 vol.% H_2O_2, 40 °C, **b** 2/20 S/L, 2 M MSA + 1 vol.% H_2O_2, and **c** MSA + 1 vol.% H_2O_2, 1/20 S/L, 40 °C

Acid concentration demonstrated a generally positive effect on the extraction of metals, with a progressive increase in leaching efficiency observed for all investigated elements except Cu. Among the elements studied, the most notable improvements were observed for Cr and lead Pb, both of which responded significantly to increasing acid concentration, indicating enhanced solubility under more acidic conditions. In contrast, Cu displayed the least sensitivity to further acid concentration increases, as its extraction efficiency had already reached approximately 93% at 2 M. This indicates that Cu was effectively leached at moderate acid strength, and higher concentrations did not provide considerable benefits.

The repeatability of the leaching experiments was evaluated by performing four parallel tests at the central conditions (2 M MSA, 1/20 S/L ratio, 40 °C, 1 vol.% H_2O_2) on Ash E. The mean values of extraction efficiencies and standard deviations are presented in Fig. 3. One of the replicates consistently showed low Cu concentrations up to the 3-h mark, leading to a substantial increase in data variability (Fig. 3a). Given the high complexity of the material and the focus on trace elements, it is challenging to definitively attribute such deviations to either analytical anomalies or inherent sample heterogeneity. Therefore, the results are evaluated using both the complete set of four replicates and a refined dataset excluding the deviating replicate, as illustrated in Fig. 3b.

In Fig. 3a, Cu exhibited considerable variation between parallels before the 4-h mark, as indicated by the large error bars at 0.5–3 h. This suggests inconsistent leaching behavior, likely due to heterogeneity in the Cu-containing phases or kinetic factors influencing the early stages of the reaction. Some forms of Cu (e.g., $CuCl_2$ or surface- adsorbed Cu) may dissolve readily during leaching, while other forms (e.g., CuO or Cu in silicate matrices) are less soluble and require longer leaching times to release. In general, standard deviations were more pronounced for all elements before the 4-h mark, indicating stronger kinetic influences during the initial stages of the leaching process. Such effects are common in the early phase of heterogeneous leaching systems, particularly when diffusion, surface reactivity, and local pH conditions fluctuate before reaching equilibrium. Notably, Cr exhibited relatively high standard deviation across all time points, which may be attributed to its presence in multiple oxidation states or association with phases of varying solubility and stability. When the replicate considered as an anomaly was excluded (Fig. 3b), the variation in Cu concentrations observed prior to the 4-h mark decreased notably, indicating that this replicate significantly contributed to the overall dispersion in the data. However, a relatively high degree of variation persisted before the 3-h point, which may be attributed to the early-stage kinetics of Cu dissolution. For the other elements, the exclusion of the same replicate did not result in substantial changes to the overall trend or

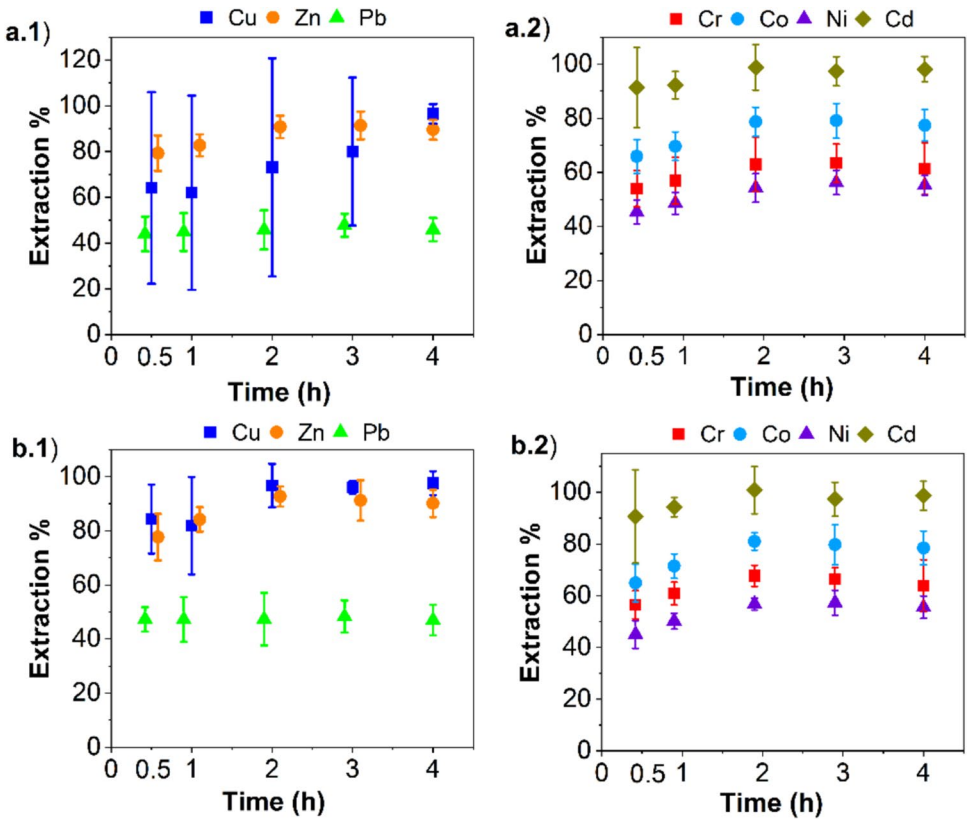

Fig. 3 Mean concentrations and standard deviations of (a1, b1) Cu, Zn, and Pb (with slight horizontal offsets applied before the 4-h mark to minimize error bar overlap) and (a2, b2) Cr, Co, Ni, and Cd over time, based on **a** four replicate experiments and **b** three replicate experiments with outlier removal. All experiments were conducted under the central leaching conditions (2 M MSA, 1/20 S/L ratio, 40 °C, 1 vol.% H_2O_2) using Ash E

variability. This suggests that the anomalous behavior was element-specific, possibly linked to the mineralogical form or distribution of Cu in that particular sub-sample.

In full quantitative ICP-MS, errors are typically in the range of maximum 10% [47]. However, in complex materials like MSWI fly ash, matrix effects and interferences can increase error levels. High concentrations of certain elements may cause signal suppression and drift, which can be mitigated by sample dilution [48]. In this study, liquid samples were diluted 100-fold to reduce such effects. Spectral interferences also affect accuracy, especially for elements with lower atomic mass like Cu and Zn (masses ~ 63–68), which are more susceptible to polyatomic interferences than higher atomic mass elements like Pb (mass ~ 208) [49]. To address this, solid ash samples were analyzed using high-resolution ICP-MS (HR-ICP-MS), which improves accuracy by resolving overlapping ions [50]. This is particularly effective in complex matrices like MSWI fly ash. Matrix-matched calibration is another effective strategy to reduce plasma-related matrix effects; however, due to the strong variability among MSWI FA/APC matrices and the lack of suitable certified reference materials across all analytes, it was not applied here. Overall, analytical errors were minimized through sample dilution and the use of HR-ICP-MS. Therefore, the variations are primarily attributed to sample complexity. According to a previous study, elemental concentration variations of MSWI FA/APC for Cu, Zn, and Pb range from 22 to 41%, depending on incineration technology, season, and region. Notably, fluidized bed plants, like that for ash E, showed particularly high variations for Cu (32%) and Pb (41%) [12].

To explore the underlying leaching mechanisms, several widely used kinetic models were evaluated, including the shrinking core model, surface reaction control, chemical reaction control, diffusion through the product layer, and mixed-control models. These approaches are commonly applied to interpret leaching kinetics in complex solid–liquid systems. However, the fitting results were inconclusive, and no single model adequately described the experimental data across all conditions (Figure S1, Table S3). The chemically diverse and heterogeneous nature of MSWI fly ash, which may involve simultaneous and competing dissolution pathways, complicates the identification of a single rate-controlling mechanism.

Figure 4 illustrates the average extraction efficiency and standard deviation at the 4-h mark based on four parallel experiments, where results indicate that the system variation minimized. Among the investigated elements, Cd, Cu, and Zn exhibited the highest extraction efficiencies, reaching 98.18 ± 4.7%, 96.47 ± 4.3%, and 89.52 ± 4.3%, respectively. In contrast, Pb extraction remained relatively low at 45.89 ± 5.1%, indicating limited solubility of Pb-bearing compounds. Other elements resulted in higher extraction

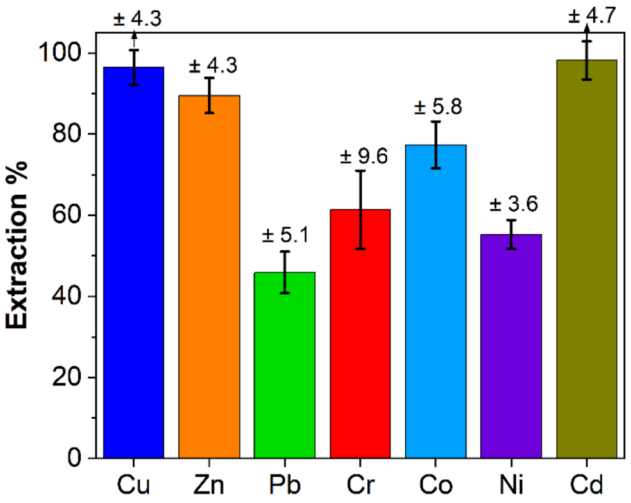

Fig. 4 Average extraction and standard deviation of Cu, Zn, Pb, Cr, Co, Ni, and Cd across four parallel experiments at 4-h mark under the central conditions (2 M MSA, 1/20 S/L ratio, 40 °C, 1 vol.% H_2O_2), conducted on Ash E

efficiencies compared to coper, with Cr and Co showing higher variation. This suggests greater sensitivity to sample heterogeneity or potential kinetic limitations in their dissolution behavior.

Overall, the differences in leaching behavior of Cu, Zn, and Pb from MSWI fly ash can be primarily attributed to their chemical speciation, which governs their mobility under acidic conditions. In addition to the commonly reported compounds identified by XANES in the literature, the widely adopted sequential extraction method [51] categorizes metals in MSWI fly ash into five operationally defined fractions: water-soluble/exchangeable (F1), acid-soluble (F2), reducible (F3), oxidizable (F4), and residual (F5). Cu is commonly associated with the acid-soluble (~ 45%) and oxidizable (~ 28%) fractions, typically present as $CuSO_4$, CuO, or metallic Cu, which explains its variable extraction depending on oxidant addition and reaction time. Upon water washing, a slight decrease in the acid-soluble fraction and an increase in the residual fraction suggest partial transformation into more stable forms [52, 53]. Zn, predominantly found in the acid-soluble fraction (~63%), remains highly leachable due to its occurrence as $ZnCl_2$ or $ZnCO_3$, which are stable in this form even after washing (~ 55–60%) [53, 54]. This accounts for the consistently high and stable Zn extraction observed under all conditions. Pb is initially concentrated in the acid-soluble fraction (F2, 48%); however, water washing reduces this association from 48% in raw FA to approximately 40% [54], which accounts for its limited extraction.

Different Ash Types

Figure 5 presents the extraction % of the elements across different ash types under central leaching conditions (2 M MSA + 1 vol.% H_2O_2, 40 °C, 1/20 solid-to-liquid ratio), based on relative extraction efficiencies. Cu extraction was relatively consistent among the ashes, with the highest values observed in Ash B and C with > 99.9%, while Ash A exhibited the lowest (76.3%). A similar trend was observed for Zn, with Ash B and C showing the highest extraction efficiencies (> 99.9%), suggesting comparable leachability of Zn and Cu across the samples. The element heat maps based on scanning electron microscopy- automated mineralogy (Fig. S2) revealed Zn and Fe integrated into the matrix phase. Zn was associated with Fe in Ashes A and D, while this association was less pronounced in Ash B, likely contributing to the lower Zn extraction rate in Ash A (73.1%) and Ash D (84.8%). SEM-AM images could not detect Cu in the analyzed agglomerates, potentially due to the low concentration and heterogenous distribution of copper in ash particles. Although the detected percentage of areas was extremely low, Cu-containing phases were successfully identified in most samples through complete area scanning with SEM-AM (Tab. A.2). Cu is associated with Ca–O–Al phases and appeared as Al–Cu in both Ash D and Ash E.

Pb showed more pronounced variation, with Ash C yielding the highest extraction (61.9%), followed by Ash D and Ash E with ~ 43% extraction, while Ash A was markedly lower (48.5%), indicating less soluble Pb phases. Cr leaching was the most efficient in Ash B with > 99.9%, whereas Ash A showed notably lower value (13.4%). Ni extraction was again highest in Ash B, followed by moderate values in Ash D (56.9%) and Ash E (54.2%). Overall, the results indicate that MSA + H_2O_2 leaching system is broadly effective across a wide range of trace metals and ash matrices. For economically valuable elements such as Cu and Zn, leaching efficiencies were consistently high across all ash types. For other elements like Pb, Ni, and Cr, the extraction efficiency showed stronger dependency on ash type, likely reflecting differences in metal speciation or phase associations.

Prospects on Future Use of MSA Leachate

Figure 6 presents the leachates from various ash samples after 4 h of leaching under central conditions, while Table 5 provides the final solution compositions for all five ash samples. The solubility of elements other than the target metals (Cu, Zn, and Pb) in MSA leachates reveals important considerations for both process selectivity and downstream treatment. Bulk elements like S and Ca are present in extremely high concentrations, particularly S, which exceeds 40,000 ppm in all samples. The concentrations of Na, K, and Mg are also considerable. Fe concentrations often surpass those of Cu, Pb, and sometimes Zn, impacting process selectivity and downstream metal recovery due to potential complexation, precipitation, or adsorption effects. The oxidation state of Fe critically influences its removal strategy: Fe^{3+} is commonly precipitated as jarosite or hydroxide

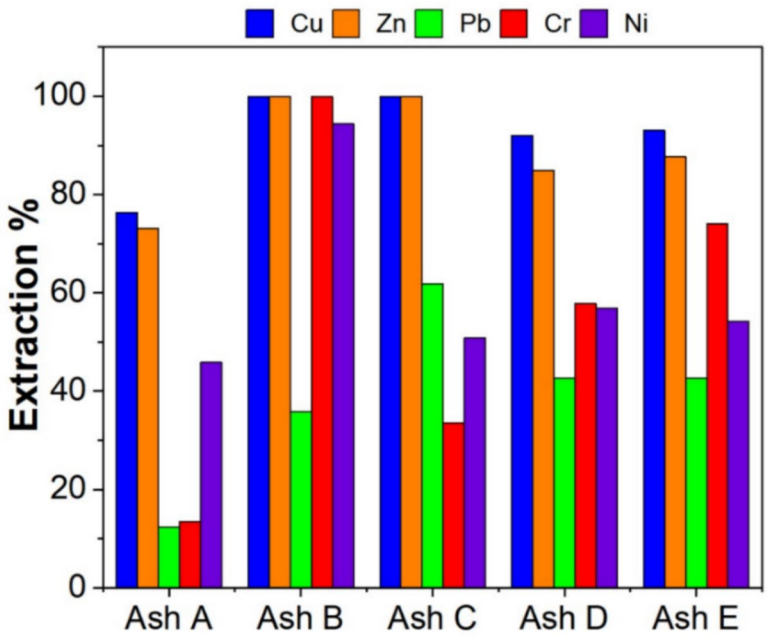

Extraction %

	Cu	Zn	Pb	Cr	Ni
Ash A	76.3	73.1	12.4	13.4	45.8
Ash B	>99.9	>99.9	35.8	>99.9	94.4
Ash C	>99.9	>99.9	61.9	33.5	50.8
Ash D	92.0	84.8	42.7	57.8	56.9
Ash E	93.1	87.7	42.7	74.0	54.2

Fig. 5 Extraction trends of Cu, Zn, Pb, Cr, and Ni for different ashes under central leaching conditions (2 M MSA + 1 vol.% H_2O_2, 40 °C, 1/20 solid-to-liquid ratio)

Fig. 6 Leach solutions of different ash samples after 4 h leaching under central leaching conditions (2 M MSA, 40 °C, 1/20 solid-to-liquid ratio). From left to right solutions are in the order of Ash A, Ash B, Ash C, Ash D, and Ash E

Table 5 Solution composition of 5 ash samples after 4-h leaching measured by ICP-MS

		Ash A ppm	Ash B	Ash C	Ash D	Ash E
Bulk/matrix elements	S	41,500	48,500	52,500	52,700	49,800
	Ca	2730	14,000	13,900	9390	11,600
	Al	801	1110	1460	1160	6040
	Si	536	1820	1760	2260	2580
	Mg	394	675	726	915	1050
	P	3950	359	375	475	269
Heavy metals/ trace elements	Fe	571	513	504	356	599
	Cu	229	55	69.4	40.5	367
	Zn	1900	674	841	933	292
	Na	3000	156	148	205	204
	Ti	106	153	137	178	164
	K	913	166	115	200	94.4
	Pb	50.8	38.7	49.5	53.4	64
	Mn	108	35.3	45.2	43.4	54.4
	Sb	1.4	23.3	43.4	45.0	17.3
	Cr	24.1	8.6	5.2	5.1	10.3
	Sn	1.7	16.5	18.9	3.6	7.6
	Ba	28.7	5.2	4.5	3.0	7.4
	Ni	48.1	3.3	4.5	2.8	4.2
	Co	9.4	0.8	1.3	1.0	3.5
	Cd	2.0	10.7	15.9	3.1	2.6

directly, whereas Fe^{2+} requires oxidation to Fe^{+3} prior to precipitation. The distinct orange coloration observed in the leachate from Ash D (Fig. 6) likely indicates the presence of Fe^{3+} species, which exhibit yellow to orange hues. In contrast, the colorless appearance of leachates from Ash A–C, and the slight green tint observed in Ash E, may suggest the dominance of Fe^{2+} species or the presence of transition metal ions like Ni^{2+} or Cr^{3+}, whose coordination complexes can contribute green coloration. The complex nature of ash samples complicates definitive conclusions regarding the oxidation of Fe^{2+} in Ash D. However, one can argue that limited competing oxidation reactions such as those involving Cu, Mn, or Cr result in a higher availability of H_2O_2 in the system, facilitating the oxidation of Fe^{2+} to Fe^{3+} in Ash D. This is supported by the relatively lower initial copper

content and final copper extraction observed in Ash D compared to other samples.

The resulting MSA leachate resembles sulfuric acid but retains Pb in solution, enhancing its recovery potential. Due to MSA's high acidity, ionic strength, and non-volatile nature, the leachate is highly conductive, making it well-suited for direct electrowinning (EW) with minimal pre-treatment. MSA has a wide electrochemical window, extending on a platinum working electrode from about − 2 V to + 2 V versus the standard hydrogen electrode (SHE). The conductivity of the MSA solutions ranged from 0.25 to 0.34 S/cm (Table 6). Although direct comparison is limited due to differences in ionic composition, previously reported conductivities for HCl and H_2SO_4 were 0.35 and 0.44 S/cm, respectively [55]. These comparable values suggest that MSA possesses suitable conductivity for electro-winning applications, requiring minimal pre-treatment. Unlike HCl and HNO_3, which can release hazardous chlorine or nitrogen oxides during EW, MSA-based systems typically evolve only oxygen at the anode, significantly improving process safety and environmental performance.

In multi-metal systems, iron must be removed prior to EW due to its high reduction potential (+ 0.77 V vs SHE), which can lead to co-deposition with copper or cathodic contamination through reduction. As previously noted, Fe^{2+} must first be oxidized to Fe^{3+} to enable selective precipitation. This can be achieved by adjusting the pH with bases such as NaOH or NH_4OH, which effectively removes iron from solution. Importantly, this process does not degrade MSA, since the hydroxide ions react only with free protons, leaving the methanesulfonate anion ($CH_3SO_3^-$) intact and preserving the acid for reuse. Once Fe is removed, sequential electrowinning of Cu, Zn, and Pb becomes feasible, though Zn recovery remains more energy-intensive due to its more negative reduction potential (− 0.76 V vs SHE), often requiring additives to suppress hydrogen evolution and prevent Zn re-dissolution. Thus, removing Cu and Pb through sequential electrowinning and precipitating Zn as a separate step can be considered. Elements like Na, K, and Mg are highly electropositive and will not plate out under typical EW conditions, so they do not interfere. Al^{3+} and Si are also unlikely to deposit due to their very negative or complex reduction pathways. However, transition metals like Mn, Sb, Cr, and Sn may co-deposit or interfere if present in higher concentrations or if plating conditions (e.g., voltage, pH) are not tightly controlled. Their effect is usually minimal at low concentrations but should still be monitored.

Table 6 Final pH and conductivity values of leach solutions after 4-h leaching under central leaching conditions (2 M MSA, 40 °C, 1/20 solid-to-liquid ratio)

	pH	Conductivity (S/cm)
Ash A	< 1	0.33
Ash B	< 1	0.28
Ash C	< 1	0.27
Ash D	< 1	0.34
Ash E	< 1	0.25

Following metal recovery, MSA can be regenerated by dosing the solution with H_2SO_4, which precipitates Ca, residual Pb and Ba (in the case of Ash A) as their insoluble sulfates, effectively releasing the sulfonic acid back into solution. Even though other bulk elements and some trace elements such as Mn, Sb, Cr, and Sn will stay in the solution, purified MSA can potentially be used for ash leaching again. This nearly closed-loop regeneration significantly reduces the need for fresh acid input and enhances the economic and environmental sustainability of the process. Although MSA is not as inexpensive as sulfuric acid, its cost is competitive with other bulk organic chemicals and possess operational advantages such as high solution conductivity and safer process integration.

Conclusion

This study provides important insights into the applicability of MSA leaching, advancing the current understanding of organic acid applications for metal recovery from MSWI FA/APC. The results demonstrate the strong potential of MSA as a greener and less corrosive alternative to traditional mineral acids, achieving over 89% extraction efficiency for key metals such as Cu and Zn. These outcomes are particularly noteworthy when compared to the conventional FLUWA process, which achieves significantly lower recoveries—around 30% for Cu and 67% for Zn. A key conclusion is that the speciation of metals within the ash matrix critically influences leaching efficiency, underscoring the importance of characterization of ash samples prior to leaching.

Although MSA may currently involve higher initial costs compared to more established leaching agents, its technical advantages and favorable environmental profile offer compelling justification for its use. Nevertheless, to support its industrial adoption, it is essential to address cost-related concerns through process optimization. While MSA is non-corrosive and ongoing developments in its production and regeneration are promising, comprehensive economic analyses are needed to evaluate its full-scale feasibility.

Future work should prioritize refining operational parameters for different ash types, not only to improve extraction efficiency but also to reduce operational costs. Additionally, integrating MSA leaching with downstream processes like electrowinning could significantly enhance the economic viability of recovering high-value metals. Reusability of purified MSA as proposed in the paper should experimentally be studied. Pilot-scale testing, continuous system

development, and detailed techno-economic assessments will be vital for transitioning MSA-based leaching from the laboratory to industry.

Supplementary Information The online version contains supplementary material available at https://doi.org/10.1007/s40831-025-01298-7.

Acknowledgements We acknowledge Laurentius Tijhuis from the Chemical and Mineralogical Laboratory at the Department of Geosciences, Norwegian University of Science and Technology, for conducting the ICP-MS analysis. The project (ASKEPOTT – Utnyttelse av verdiskapingspotensialet i flyveaske og svovelsyre) has received funding from the Norwegian Research Council (Project number: 332144).

Author Contributions Edzhe Soylu: conceptualization, methodology, investigation, writing—original draft. Linus Meistad: methodology, investigation, writing- reviewing and editing. Elif Emil-Kaya: conceptualization, methodology, supervision, writing—reviewing and editing. Kai Erik Ekstrøm: funding acquisition, writing—reviewing and editing. Inge Johansson: funding acquisition, writing—reviewing and editing. Przemyslaw B. Kowalczuk: writing—reviewing and editing. Gabriella Tranell: methodology, conceptualization, supervision, writing—reviewing and editing.

Funding Open access funding provided by NTNU Norwegian University of Science and Technology (incl St. Olavs Hospital - Trondheim University Hospital). This work was funded by Norges Forskningsråd, 332144.

Declarations

Conflict of interest On behalf of all authors, the corresponding author states that there is no conflict of interest.

References

1. Kaza S, Yao L, Bhada-Tata P, Woerden FV (2018) What a waste 2.0: a global snapshot of solid waste management to 2050. World Bank, Washington DC
2. Zhang Y, Wang L, Chen L, Ma B, Zhang Y, Ni W, Tsang DCW (2021) Treatment of municipal solid waste incineration fly ash: state-of-the-art technologies and future perspectives. J Hazard Mater 411:125132. https://doi.org/10.1016/j.jhazmat.2021.125132
3. Tammemagi H (2000) Incineration: the burning issue. In: Tammemagi H (ed) The waste crisis: landfills, incinerators, and the search for a sustainable future. Oxford University Press, Oxford
4. Neuwahl F, Cusano G, Gomez Benavides J, Holbrook S, Roudier S (2019) Best Available Techniques (BAT) reference document for waste incineration: Industrial Emissions Directive 2010/75/EU (Integrated Pollution Prevention and Control), Publications Office, LU. https://data.europa.eu/doi/https://doi.org/10.2760/761437. Accessed 16 May 2024
5. Leckner B, Lind F (2020) Combustion of municipal solid waste in fluidized bed or on grate – a comparison. Waste Manag 109:94–108. https://doi.org/10.1016/j.wasman.2020.04.050
6. Ajorloo M, Ghodrat M, Scott J, Strezov V (2022) Heavy metals removal/stabilization from municipal solid waste incineration fly ash: a review and recent trends. J Mater Cycles Waste Manag 24:1693–1717. https://doi.org/10.1007/s10163-022-01459-w
7. Pan Y, Wu Z, Zhou J, Zhao J, Ruan X, Liu J, Qian G (2013) Chemical characteristics and risk assessment of typical municipal solid waste incineration (MSWI) fly ash in China. J Hazard Mater 261:269–276. https://doi.org/10.1016/j.jhazmat.2013.07.038
8. Ma X, He T, Da Y, Xu Y, Wan Z (2023) Physical properties, chemical composition, and toxicity leaching of incineration fly ash by multistage water washing. Environ Sci Pollut Res 30:80978–80987. https://doi.org/10.1007/s11356-023-28170-z
9. Li W, Gu K, Yu Q, Sun Y, Wang Y, Xin M, Bian R, Wang H, Wang Y, Zhang D (2021) Leaching behavior and environmental risk assessment of toxic metals in municipal solid waste incineration fly ash exposed to mature landfill leachate environment. Waste Manag 120:68–75. https://doi.org/10.1016/j.wasman.2020.11.020
10. Nagib S, Inoue K (2000) Recovery of lead and zinc from fly ash generated from municipal incineration plants by means of acid and or alkaline leaching. Hydrometallurgy 56:269–292. https://doi.org/10.1016/S0304-386X(00)00073-6
11. Liu J, Xie G, Wang Z, Zeng C, Fan X, Li Z, Ren J, Xing F, Zhang W (2023) Manufacture of alkali-activated cementitious materials using municipal solid waste incineration (MSWI) ash: immobilization of heavy metals in MSWI fly ash by MSWI bottom ash. Constr Build Mater 392:131848. https://doi.org/10.1016/j.conbuildmat.2023.131848
12. Nedkvitne EN, Borgan Ø, Eriksen DØ, Rui H (2021) Variation in chemical composition of MSWI fly ash and dry scrubber residues. Waste Manag 126:623–631. https://doi.org/10.1016/j.wasman.2021.04.007
13. European Parliament and Council (2018) Directive (EU) 2018/ of the European Parliament and of the Council of 30 May 2018 amending Directive 1999/31/EC on the landfill of waste, European Commission
14. Fabricius A-L, Renner M, Voss M, Funk M, Perfoll A, Gehring F, Graf R, Fromm S, Duester L (2020) Municipal waste incineration fly ashes: from a multi-element approach to market potential evaluation. Environ Sci Eur 32:88. https://doi.org/10.1186/s12302-020-00365-y
15. Decision-2003/33-EN-EUR-Lex, (n.d.). https://eur-lex.europa.eu/eli/dec/2003/33(1)/oj/eng. Accessed 3 Jan 2025
16. Wang H, Zhu F, Liu X, Han M, Zhang R (2021) A mini-review of heavy metal recycling technologies for municipal solid waste incineration fly ash. Waste Manag Res 39:1135–1148. https://doi.org/10.1177/0734242X211003968
17. Rissler J, Klementiev K, Dahl J, Steenari B-M, Edo M (2020) Identification and quantification of chemical forms of Cu and Zn in MSWI ashes using XANES. Energy Fuels 34:14505–14514. https://doi.org/10.1021/acs.energyfuels.0c02226
18. Rissler J, Fedje KK, Klementiev K, Ebin B, Nilsson C, Rui HM, Klufthaugen TM, Sala S, Johansson I (2024) Zinc speciation in fly ash from MSWI using XAS - novel insights and implications. J Hazard Mater 477:135203. https://doi.org/10.1016/j.jhazmat.2024.135203
19. Nedkvitne EN, Eriksen DØ, Omtvedt JP (2023) Grade and tonnage comparison of anthropogenic raw materials and ores for Cu, Zn, and Pb recovery. Resources 12:33. https://doi.org/10.3390/resources12030033

20. Weibel G (2017) Optimized metal recovery from fly ash from municipal solid waste incineration, Doctoral Thesis, Universität Bern. http://boristheses.unibe.ch/861/. Accessed 1 Apr 2025
21. Weibel G, Eggenberger U, Kulik DA, Hummel W, Schlumberger S, Klink W, Fisch M, Mäder UK (2018) Extraction of heavy metals from MSWI fly ash using hydrochloric acid and sodium chloride solution. Waste Manag 76:457–471. https://doi.org/10.1016/j.wasman.2018.03.022
22. Zucha W, Weibel G, Wolffers M, Eggenberger U (2020) Inventory of MSWI fly ash in Switzerland: heavy metal recovery potential and their properties for acid leaching. Processes 8:1668. https://doi.org/10.3390/pr8121668
23. Liu R, Tian Z, Cheng H, Zhou H, Wang Y (2021) Organic acid leaching was an efficient approach for detoxification of metal-containing plant incineration ash. Environ Sci Pollut Res 28:32721–32732. https://doi.org/10.1007/s11356-021-13027-0
24. Wu H-Y, Ting Y-P (2006) Metal extraction from municipal solid waste (MSW) incinerator fly ash—chemical leaching and fungal bioleaching. Enzyme Microb Technol 38:839–847. https://doi.org/10.1016/j.enzmictec.2005.08.012
25. Gernon MD, Wu M, Buszta T, Janney P (1999) Environmental benefits of methanesulfonic acid. Green Chem 1:127–140. https://doi.org/10.1039/a900157c
26. Binnemans K, Jones PT (2023) Methanesulfonic acid (MSA) in hydrometallurgy. J Sustain Metall 9:26–45. https://doi.org/10.1007/s40831-022-00641-6
27. Palden T, Onghena B, Regadío M, Binnemans K (2019) Methanesulfonic acid: a sustainable acidic solvent for recovering metals from the jarosite residue of the zinc industry. Green Chem 21:5394–5404. https://doi.org/10.1039/C9GC02238D
28. Jadhao PR, Mishra S, Singh A, Pant KK, Nigam KDP (2023) A sustainable route for the recovery of metals from waste printed circuit boards using methanesulfonic acid. J Environ Manage 335:117581. https://doi.org/10.1016/j.jenvman.2023.117581
29. Ahn J, Wu J, Lee J (2019) Investigation on chalcopyrite leaching with methanesulfonic acid (MSA) and hydrogen peroxide. Hydrometallurgy 187:54–62. https://doi.org/10.1016/j.hydromet.2019.05.001
30. Wu Z, Dreisinger DB, Urch H, Fassbender S (2014) Fundamental study of lead recovery from cerussite concentrate with methanesulfonic acid (MSA). Hydrometallurgy 142:23–35. https://doi.org/10.1016/j.hydromet.2013.10.018
31. Caviglia C, Destefanis E, Pastero L, Bernasconi D, Bonadiman C, Pavese A (2022) MSWI fly ash multiple washing: kinetics of dissolution in water, as function of time, temperature and dilution. Minerals 12:742. https://doi.org/10.3390/min12060742
32. Meer I, Nazir R (2018) Removal techniques for heavy metals from fly ash. J Mater Cycles Waste Manag 20:703–722. https://doi.org/10.1007/s10163-017-0651-z
33. Luo H, Cheng Y, He D, Yang E-H (2019) Review of leaching behavior of municipal solid waste incineration (MSWI) ash. Sci Total Environ 668:90–103. https://doi.org/10.1016/j.scitotenv.2019.03.004
34. Soylu E, Lode S, Silva CM, Simavik KR, Ekstrøm KE, Johansson I, Sørensen BE, Kowalczuk PB, Tranell G (2025) Comprehensive characterization of solid waste incineration fly ash before and after salt washing: evaluating analytical methods for sustainable waste management. Resour Conserv Recycl Adv 27:200268. https://doi.org/10.1016/j.rcradv.2025.200268
35. Binnemans K, Jones PT (2024) Methanesulfonic acid (MSA) in clean processes and applications: a tutorial review. Green Chem 26:8583–8614. https://doi.org/10.1039/D4GC02031F
36. Hsiao MC, Wang HP, Wei YL, Chang J-E, Jou CJ (2002) Speciation of copper in the incineration fly ash of a municipal solid waste. J Hazard Mater 91:301–307. https://doi.org/10.1016/S0304-3894(02)00015-8
37. Lassesson H, Fedje KK, Steenari B-M (2014) Leaching for recovery of copper from municipal solid waste incineration fly ash: influence of ash properties and metal speciation. Waste Manag Res 32:755–762. https://doi.org/10.1177/0734242X14542147
38. Lassesson H, Steenari B-M (2013) Speciation of copper in ash from a fluidized-bed boiler fired with municipal solid waste. Energy Fuels 27:3891–3897. https://doi.org/10.1021/ef400386j
39. Tuan Y-J, Wang HP, Chang J-E, Chao C-C, Tsai C-K (2010) Speciation of copper in the thermally stabilized slag. Nucl Instrum Methods Phys Res Sect A Accel Spectrom Detect Assoc Equip 619:316–318. https://doi.org/10.1016/j.nima.2010.01.023
40. Kitamura H, Dahlan AV, Tian Y, Shimaoka T, Yamamoto T, Takahashi F (2020) Application of micro-scale correlation analysis to estimate metal speciation and the matrix in municipal solid waste incineration fly ash. J Mater Cycles Waste Manag 22:1081–1093. https://doi.org/10.1007/s10163-020-01001-w
41. Struis RPWJ, Ludwig C, Lutz H, Scheidegger AM (2004) Speciation of zinc in municipal solid waste incineration fly ash after heat treatment: an X-ray absorption spectroscopy study. Environ Sci Technol 38:3760–3767. https://doi.org/10.1021/es0346126
42. Takaoka M, Yamamoto T, Tanaka T, Takeda N, Oshita K, Uruga T (2005) Direct speciation of lead, zinc and antimony in fly ash from waste treatment facilities by XAFS spectroscopy. Phys Scr. https://doi.org/10.1238/Physica.Topical.115a00943
43. Tian S, Zhu Y, Meng B, Guan J, Nie Z, Die Q, Xu W, Yu M, Huang Q (2018) Chemical speciation of lead in secondary fly ash using X-ray absorption spectroscopy. Chemosphere 197:362–366. https://doi.org/10.1016/j.chemosphere.2018.01.026
44. Sundramurthy VP, Rajoo B, Srinivasan NR, Kavitha R (2020) Bioleaching of Zn from sphalerite using *Leptospirillum ferriphilum* isolate: effect of temperature and kinetic aspects. Appl Biol Chem 63:44. https://doi.org/10.1186/s13765-020-00528-8
45. Mubarok MZ, Sukamto K, Ichlas ZT, Sugiarto AT (2018) Direct sulfuric acid leaching of zinc sulfide concentrate using ozone as oxidant under atmospheric pressure. Minerals Metall Process 35:133–140. https://doi.org/10.19150/mmp.8462
46. Fassbender S, Dreisinger D, Wu Z (2014) Recovering lead from a mixed oxidized material, US20140131219A1. https://patents.google.com/patent/US20140131219A1/en. Accessed 20 Jun 2025
47. Chen H, Dabek-Zlotorzynska E, Rasmussen PE, Hassan N, Lanouette M (2008) Evaluation of semiquantitative analysis mode in ICP-MS. Talanta 74:1547–1555. https://doi.org/10.1016/j.talanta.2007.09.037
48. McCurdy E (2019) ICP-MS: essential steps to optimize matrix tolerance. 34: 31–33
49. McCurdy E, Woods G, Potter D (2006) Unmatched removal of spectral interferences in ICP-MS using the agilent octopole reaction system with Helium Collision mode application, Agilent Technologies
50. Wilschefski SC, Baxter MR (2019) Inductively coupled plasma mass spectrometry: introduction to analytical aspects. Clin Biochem Rev 40:115–133. https://doi.org/10.33176/AACB-19-00024
51. Su P, Xia M, Chen K, Wang H, Li X, Zhou Z, Zhang R, Zhang L, Zhao S (2025) Study on the solidification/stabilization of MSWI fly ash by composite alkali-activated cementitious materials. ACS Omega 10:5659–5667. https://doi.org/10.1021/acsomega.4c08962
52. Chuai X, Yang Q, Zhang T, Zhao Y, Wang J, Zhao G, Cui X, Zhang Y, Zhang T, Xiong Z, Zhang J (2022) Speciation and leaching characteristics of heavy metals from municipal solid waste incineration fly ash. Fuel 328:125338. https://doi.org/10.1016/j.fuel.2022.125338
53. Xu P, Zhao Q, Qiu W, Xue Y (2019) The evaluation of the heavy metal leaching behavior of MSWI-FA added alkali-activated materials bricks by using different leaching test methods. Int J Environ Res Public Health 16:1151. https://doi.org/10.3390/ijerph16071151

54. Bernasconi D, Caviglia C, Destefanis E, Bonadiman C, Brombin V, Mancinelli M, Tassinari R, Pavese A (2025) Steam washing for MSWI-FA treatment. Waste Manag 195:10–21. https://doi.org/10.1016/j.wasman.2025.01.031
55. Tang C, Zhou D (2012) Methanesulfonic acid solution as supporting electrolyte for zinc-vanadium redox battery. Electrochim Acta 65:179–184. https://doi.org/10.1016/j.electacta.2012.01.036